Diurnal Cycle of Convection at the ARM SGP Site: Role of Large-Scale Forcing, Surface Fluxes, and Convective Inhibition

G. J. Zhang
Center for Atmospheric Sciences
Scripps Institution of Oceanography
La Jolla, California

Introduction

Atmospheric convection undergoes strong diurnal variation over both land and oceans (Gray and Jacobson 1977; Dai 2001; Nesbitt and Zipser 2003). Because of the nature of the diurnal variation of solar radiation, the phasing of convection with solar radiation has a significant impact on the atmospheric radiation budget and cloud radiative forcing. A number of studies have investigated the possible mechanisms of the diurnal variation of convection (Gray and Jacobson 1977; Randall et al. 1991; Dai et al. 1999; Dai 2001). Yet, in regional and global climate models, the diurnal variation of convection is poorly simulated, particularly over land (Dai et al. 1999; Betts and Jacob 2002). For example, at the Southern Great Plains (SGP) site of the Atmospheric Radiation Measurement (ARM) Program, convection simulated by the National Center for Atmospheric Research (NCAR) community atmospheric model (CAM) peaks in the early afternoon, whereas observations indicate that convection reaches maximum at night.

In this study, we examine the diurnal variation of convection and convective instability, convective inhibition, large-scale forcing, surface sensible and latent heat fluxes at the ARM SGP site. The objective is to understand what the major factors are that control the diurnal variation of convection in this continental environment. The relative importance of processes contributing to the observed variations will be discussed.

Data and Analysis Method

The data are from the summer 1997 intensive operational period at the SGP site of the ARM Program. The observations cover 29 days from June 19 to July 18, 1997. They are interpolated to 20 min. intervals by the variational analysis of Zhang and Lin (1997). The vertical resolution is 50 mb starting from 965 mb and ending at 115 mb.

We use convective available potential energy (CAPE) to measure convective instability in the atmosphere, and convective inhibition (CIN [convective inhibition, the negative part of CAPE]) in the lower troposphere) to measure convective suppression. They are defined by:

$$CAPE = \int_{p_t}^{p_b} R_d (T_{vp} - \overline{T}_v) d\,ln\,p$$

and

$$CIN = \int_{p_{lfc}}^{p_b} R_d (T_{vp} - \overline{T}_v) d\,ln\,p$$

respectively, where p_b is the level in the boundary layer at which convective air parcels originate, p_{lfc} and p_t are the level of free convection and the level at which the parcel loses its buoyancy, respectively. T_v is virtual temperature, subscript p denotes parcel's property, and overbar denotes the property of the parcel's large-scale environment. Since CAPE is the vertical integral of the difference between T_v of an air parcel lifted from the boundary layer and T_v of its environment, net CAPE change consists of two parts, one due to the parcel's virtual temperature change and one due to the ambient virtual temperature change,

$$\frac{\partial CAPE}{\partial t} = \frac{\partial CAPE_{Tv}}{\partial t} + \frac{\partial CAPE_{Tvp}}{\partial t}$$

where

$$\frac{\partial CAPE_{Tv}}{\partial t} = -R_d \int_{p_t}^{p_b} \frac{\partial \overline{T}_v}{\partial t} d\,ln\,p$$

is related to virtual temperature changes in the free troposphere above the boundary layer and

$$\frac{\partial CAPE_{Tvp}}{\partial t} = R_d \int_{p_t}^{p_b} \frac{\partial T_{vp}}{\partial t} d\,ln\,p = (T_{vb} - T_{vt}) \frac{C_p \partial \theta_{eb}}{\theta_{eb} \partial t}$$

is related to the parcel's virtual temperature change, which is proportional to changes in equivalent potential temperature of the boundary layer. Here T_{vb} and T_{vt} are the virtual temperature at the parcel's initial level and the neutral buoyancy level, respectively. θ_{eb} is the equivalent potential temperature at the parcel's initial level (Emanuel et al. 1994).

Similar to the net CAPE change, partial CAPE changes resulting from the large-scale advection and surface turbulent fluxes (denoted by subscript ls) can be separated into contributions from the free-tropospheric and boundary layer changes, respectively.

$$\left(\frac{\partial CAPE}{\partial t}\right)_{ls} = \left(\frac{\partial CAPE_{Tv}}{\partial t}\right)_{ls} + \left(\frac{\partial CAPE_{Tvp}}{\partial t}\right)_{ls}$$

Observations between convective and non-convective periods are contrasted to identify factors responsible for the diurnal variation of convection. To composite the diurnal variation, each variable is averaged over convective and non-convective periods separately at each local time.

Results

Figure 1 shows the diurnal variation of CAPE, CIN, the time rate of CAPE change, and contributions to it from the free tropospheric temperature and boundary layer temperature variations, respectively. On diurnal timescale, CAPE and CIN are out of phase for both convective and non-convective periods. CAPE reaches maximum in mid-afternoon and minimum at night, while CIN is the smallest in mid-afternoon and the largest in early morning. CIN is considerably larger in non-convective periods than in convective periods, suggesting that it may play some important roles in suppressing convection. CAPE change with time reaches maximum in early afternoon and minimum near midnight for both convective and non-convective periods, and is dominated by thermodynamic changes of the boundary layer air. On the other hand, contribution to CAPE change from the free tropospheric temperature variation is only a small fraction of that due to boundary layer thermodynamic changes, with maximum occurring near 0400 LT and minimum occurring near 1500 LT. Other than CIN, these variables as well as their diurnal variations have no qualitative difference between convective and non-convective periods, thus are unlikely to be directly responsible for the diurnal variation of convection.

Figure 2 shows the diurnal variation of CAPE change due to large-scale forcing from the free troposphere and the boundary layer, respectively. Also shown are the diurnal variations of precipitation and surface sensible and latent heat fluxes. The most dramatic difference between convective and non-convective periods is the CAPE change resulting from the free tropospheric large-scale forcing. During non-convective periods, as indicated by the negligible surface precipitation, there is little change in CAPE due to the free tropospheric forcing. During convective periods, CAPE change due to free tropospheric forcing reaches a maximum near midnight and a minimum around 1000 LT. This diurnal variation is in excellent agreement with the phase of precipitation. On the other hand, there is no significant difference in the diurnal variation of the large-scale CAPE generation by the boundary layer changes between convective and non-convective periods. They are comparable in magnitude, and both reach a maximum near 1400 LT and a minimum near 0200 LT. Since the major forcing factor in the large-scale CAPE generation from the boundary layer is the surface sensible and latent heat fluxes, their variations are highly in phase with the large-scale CAPE generation by the boundary layer changes, as expected. Note that the diurnal variation of precipitation is almost out of phase with that of the CAPE generation by the boundary layer forcing, suggesting that the latter is not responsible for the diurnal variation of convection.

The thermodynamic properties of the near surface air are important to convection. This is partly reflected in Figure 1, which shows that CIN is significantly larger in non-convective periods. To further examine their roles, Figure 3 shows the diurnal variation of the near-surface equivalent potential temperature, lifting condensation level (LCL), level of free convection (LFC) and vertical velocity for convective and non-convective periods. During convective periods, surface air has the highest equivalent potential temperature and lowest LFC in early to mid-afternoon. The LCL is also close to being the lowest. In spite of these favorable conditions, maximum convection does not occur at that time. At night, although LCL and LFC are high, and surface air equivalent potential temperature is near minimum, strong upward motion of the boundary layer air apparently helps the near surface air parcels to break the CIN barrier. This together with the free tropospheric large-scale generation of CAPE makes convection reach maximum near midnight. During non-convective periods, the surface air equivalent potential temperature has smaller amplitude in diurnal variation. It also reaches the maximum later in

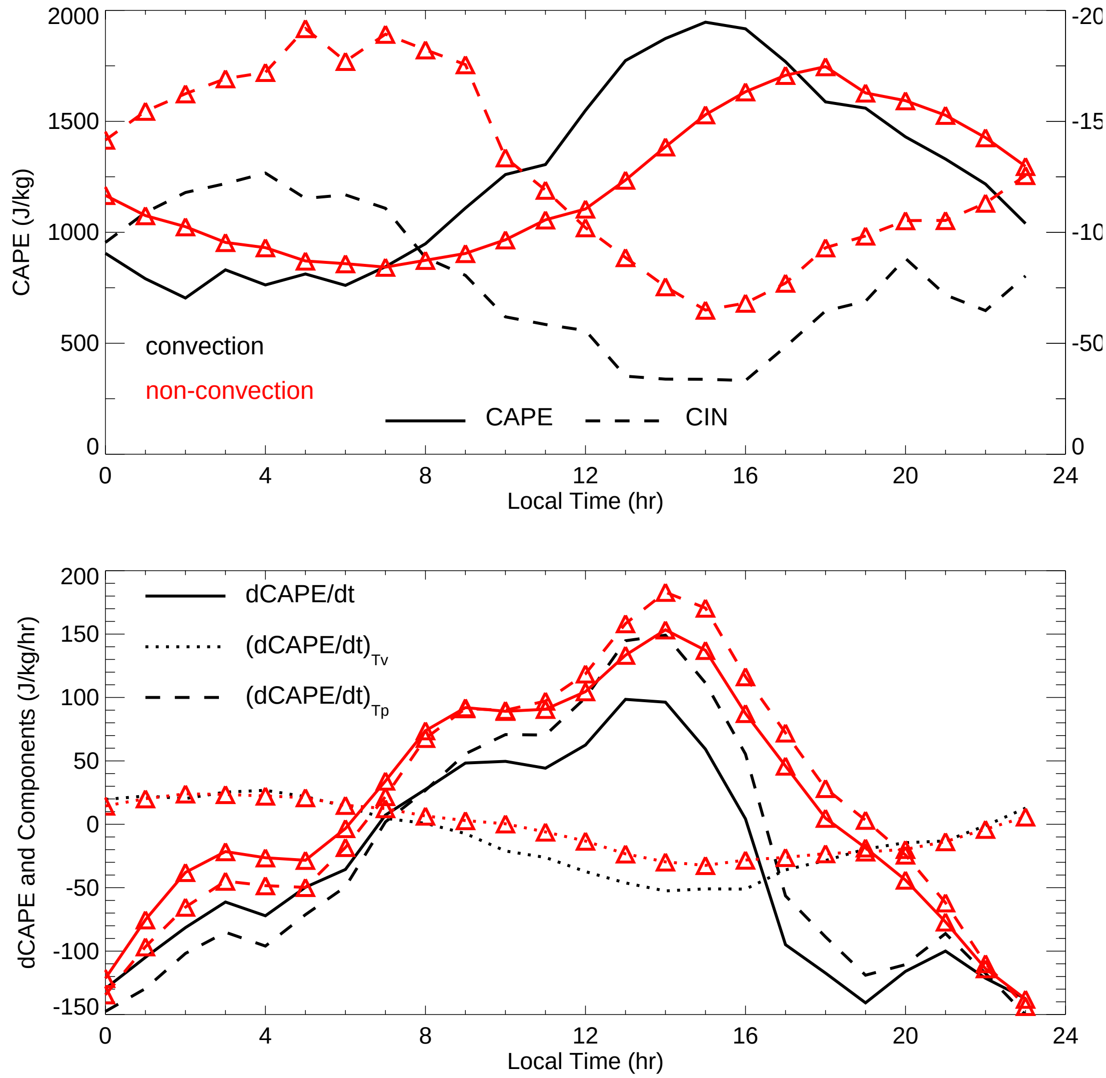

Figure 1. Diurnal variation of CAPE and CIN (top), CAPE change (solid) and contribution from parcels' (dashed) and ambient (dotted) temperature changes for convective (black) and non-convective periods (red with triangles).

the afternoon. The LCL and LFC are higher, meaning the air is drier and has deeper stable layer barrier. Furthermore, the low level vertical velocity is insignificant throughout the day, with subsidence of the time. All of these conditions make convection unfavorable.

Summary

This study examines the roles of the large-scale forcing, surface fluxes, and convective inhibition in the diurnal variation of convection using the ARM SGP data. It is found that the diurnal variation of the free tropospheric large-scale forcing has a strong phase relationship with convection, both reaching maximum near midnight and minimum before local noon. Surface sensible and latent heat fluxes generate CAPE, but this CAPE is not released by convection. Instead, it is stored in the atmosphere to

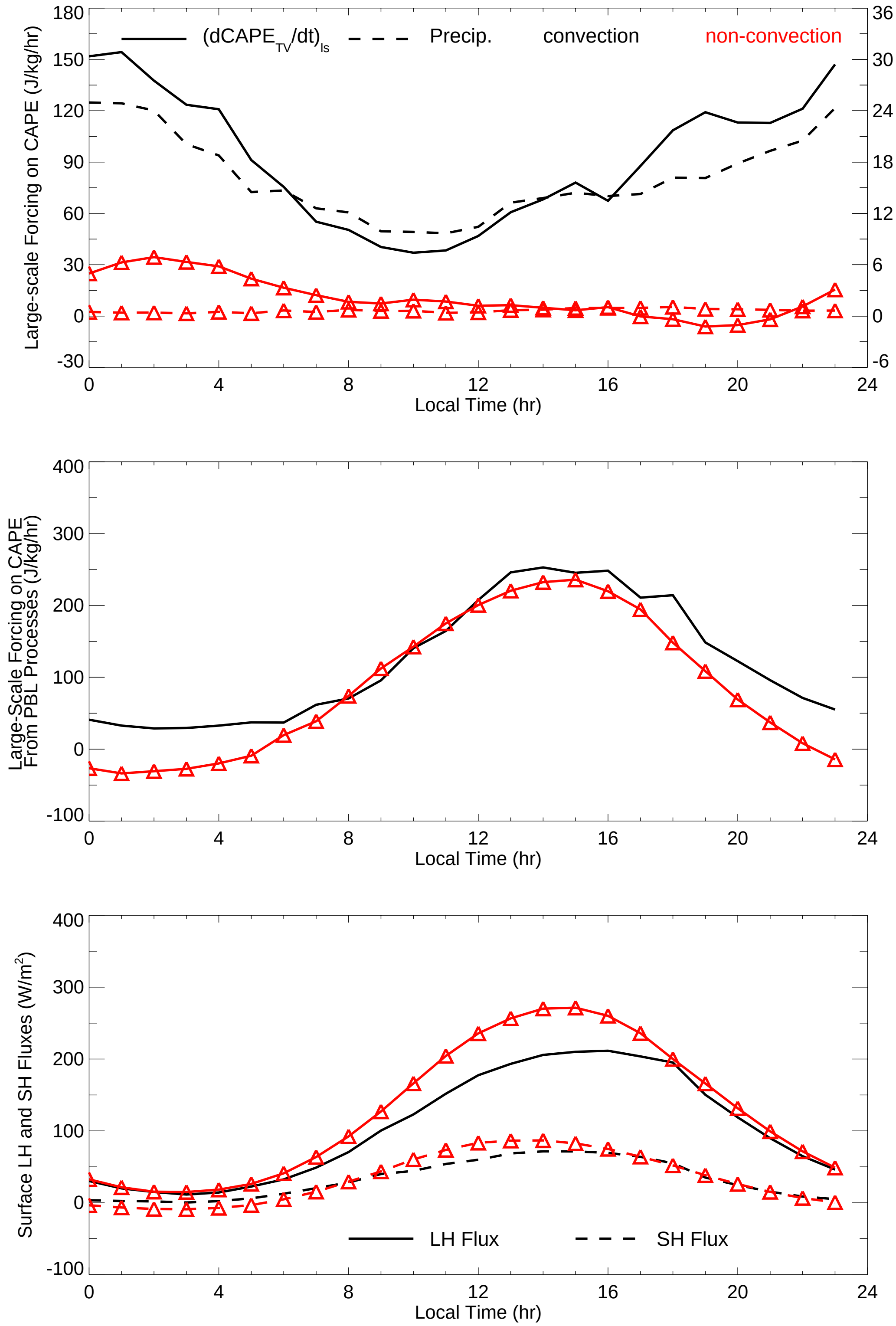

Figure 2. Diurnal variation of CAPE change due to large-scale forcing in the free troposphere and precipitation (top), CAPE change due to PBL process forcing (middle), and sensible and latent heat fluxes (bottom). Black line is for convective and red line with triangles is for non-convective periods

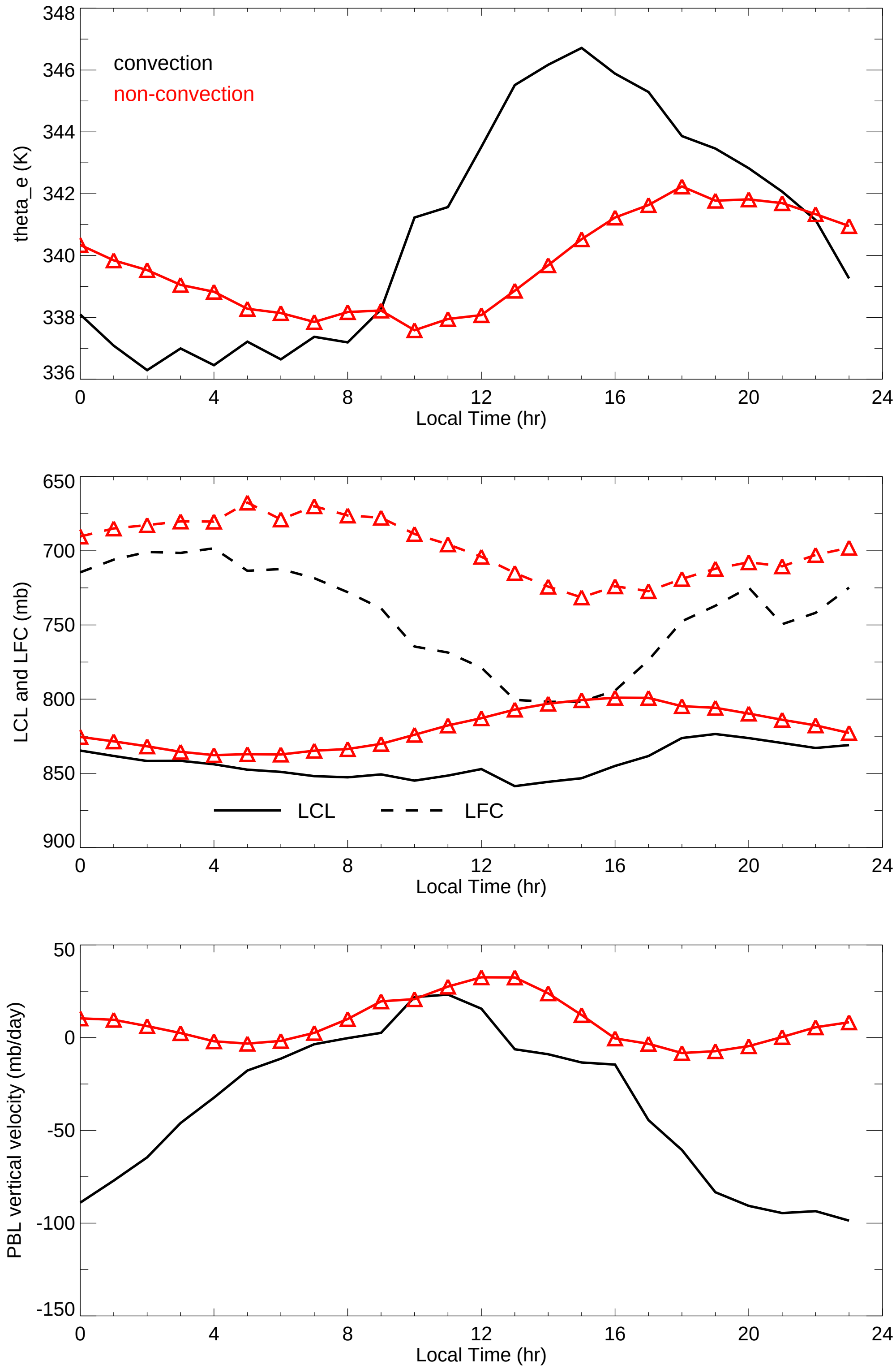

Figure 3. Diurnal variation of the near-surface air equivalent potential temperature (top), LCL and LFC (middle), and vertical velocity for convective (black) and non-convective (red with triangles) periods, respectively.

maintain the observed diurnal CAPE variation. Convective inhibition is larger in non-convective periods than in convective periods, and is in opposite diurnal phase to that of CAPE. The diurnal variation of the thermodynamic properties of the near-surface air is not well related to that of convection. The air is warmer and moister, with lower LCL and LFC, in the early to mid-afternoon, yet maximum convection does not appear until midnight when lifting of the surface air is the strongest.

References

Betts, A., and C. Jacob, 2002: Study of diurnal cycle of convective precipitation over Amazonia using a single column model. *J. Geophys. Res*., **107**, 4732, doi: 10.1029/2002JD002264.

Dai, A., 2001: Global precipitation and thunderstorm frequencies. Part II: Diurnal variations. *J. Climate*, **14**, 1112-1128.

Dai, A., F. Giorgi, and K. E. Trenberth, 1999: Observed and model simulated diurnal cycles of precipitation over the contiguous United States. *J. Geophys*. Res., **104**, 6377-6402.

Gray, W. M., and R. W. Jocobson Jr., 1977: Diurnal variation of deep cumulus convection. *Mon. Wea. Rev.,* **105**, 1171-1188.

Nesbitt, S. W., and E. J. Zipser, 2003: The diurnal cycle of rainfall and convective intensity according to three years of TRMM measurements. *J. Climate*, **16**, 1456-1475.

Randall, D. A., Harshvardhan, and D. A. Dazlich, 1991: Diurnal variability of the hydrological cycle in a general circulation model. *J. Atmos. Sci*., **48**, 40-62.

Zhang, G. J., 2002: Convective quasi-equilibrium in midlatitude continental environment and its effect on convective parameterization. *J. Geophys. Res*., **107,** doi: 10.1029/2001JD001005.

Zhang, M., and J. Lin, 1997: Constrained variational analysis of sounding data based on column-integrated budgets of mass, heat, moisture, and momentum: Approach and Application to ARM Measurements. *J. Atmos. Sci*., **54**, 1503-1524.